Enhanced heat transfer in free convection-dominated melting in a rectangular cavity with an isothermal vertical wall

Zhen-Xiang Gong [1], Sakamon Devahastin*, Arun S. Mujumdar

Department of Chemical Engineering, McGill University, 3610 University Street, Montreal, Quebec, Canada, H3A 2B2

Abstract

Free convection-dominated melting of a phase change material in a rectangular cavity with an isothermally heated vertical wall is simulated using the streamline upwind/Petrov–Galerkin finite element technique in combination with a fixed-grid primitive variable method. The enthalpy–porosity model is employed to account for the physics of the evolution of the flow at the solid/liquid interface. A penalty formulation is used to treat the incompressibility constraint in the momentum equations. Inverting of the container at an appropriate stage during the melting process is proposed as a simple but effective technique for enhancement of free convection-controlled heat transfer in the phase change material. The technique results in more than 50% increase of the energy charge rate during the melting process for some specific cases. © 1999 Elsevier Science Ltd. All rights reserved.

Keywords: Finite element method; Phase change material; Thermal energy storage

1. Introduction

Free convection-dominated melting along a heated vertical wall in a rectangular enclosure has attracted considerable research attention due to its fundamental importance in various

---

* Corresponding author. Tel.: +1-514-398-4273; fax: +1-514-398-6678.

  E-mail address: sakamon@chemeng.lan.mcgill.ca (S. Devahastin)

[1] Current address: Hyprotech Co., 300 Hyprotech Centre, 1110 Centre Street North, Calgary, Alberta, Canada T2E 2R2

Nomenclature

A	porosity function for the momentum equation
A^*	dimensionless form of A
A_{xy}	area of a computational domain
b	a small constant
c	specific heat
C	constant
f_{H}	enthalpy–temperature function
Fo	Fourier number
g_i	gravitational force vector
h	enthalpy
H	dimensionless enthalpy
k	heat conductivity
L_x	length of rectangular enclosure in x direction
L_y	length of rectangular enclosure in y direction
n_i	surface unit normal vector
p	fluid pressure
P	dimensionless fluid pressure
Pr	Prandtl number
q	heat flux
q_{a}	prescribed heat flux
q_{c}	convective heat flux
q_{r}	radiative heat flux
Q	instantaneous energy charged
Q_{T}	total energy charged
Q_{M}	maximum energy charged
Ra	Rayleigh number
s	boundary surface coordinate
Ste	Stefan number
t	time
T	temperature
T_0	reference temperature
T_{m}	melting point of PCM
T_{w}	isothermal wall temperature
u_x	velocity in x direction
u_y	velocity in y direction
u_i	velocity component
U	dimensionless velocity of x direction
V	dimensionless velocity of y direction
x, y	coordinate
X, Y	dimensionless coordinate

Greek symbols

α	diffusivity
β	expansion coefficient
θ	dimensionless temperature
θ_B	dimensionless boundary temperature
Δh	latent heat
λ	porosity of a mush zone
Γ	boundary
μ	viscosity
ρ	density
ω	the angle horizontal direction to x axis
σ_{ij}	stress tensor

Subscripts

l	liquid
s	solid
x	component of x direction
y	component of y direction

Superscript

$^-$	overbar, boundary value of the variable
0	initial value

technological applications, e.g. thermal energy storage systems. Several pioneering experimental studies in this area [1–8] have already shown the effects of natural convection on the melting heat transfer along a vertical wall in rectangular cavities. A number of numerical/analytical studies [9–15] have also been developed over the past decade based on the well-known Boussinesq's assumption.

Keller and Bergman [16] modelled numerically the steady-state melting and freezing in an open rectangular cavity including buoyancy and surface tension forces in the liquid phase. They found that surface tension-induced flow could affect the solid geometry and, ultimately, the melting and freezing rates. Bergman and Webb [17] extended Keller and Bergman's model [16] to transient melting and freezing of a pure metal. Liu et al. [18] studied both numerically and experimentally melting and solidification of a pure metal in an open cavity with liquid phase buoyancy and surface tension forces. Their numerical results were successfully verified by comparing them with the experimental ones.

Ho and Chu [19,20] simulated convection-controlled meting of *n*-octadecane contained in a vertical square enclosure subjected to a time-dependent sinusoidal oscillatory wall temperature. Later, Ho and Chu [21] simulated the coupled melting and free convection heat transfer in two vertical rectangular composite cells, one of which is filled with a PCM while the other is an air layer.

Webb and Viskanta [22] experimentally studied melting in inclined rectangular enclosures.

They reported that the effect of inclination from the vertical causes three-dimensional free convection and significantly enhances the overall melting rate. Melting of a phase change material in an inclined rectangular enclosure was also studied both experimentally and numerically by Inaba et al. [23,24].

In this paper, free convection-dominated melting of a phase change material in a rectangular cavity with an isothermally heated vertical wall is studied with the aid of the streamline upwind/Petrov–Galerkin finite element technique in combination with a fixed-grid primitive variable method to solve the governing two-dimensional conservation equations. Inverting the phase change material (PCM) container at an appropriate stage during the melting process is proposed and simulated as a simple but effective technique for enhancement of free convection-controlled heat transfer in the phase change material. Simulations were carried out to investigate the effects of different parameters on the enhancement of the heat transfer rate by inverting the PCM container. Sample results are presented and discussed.

2. Mathematical formulation

For the mathematical description of a melting or freezing process, the following assumptions are made: (1) heat transfer in the PCM is conduction/convection controlled, and the melt is Newtonian and incompressible; (2) the flow in the melt is laminar and viscous dissipation is negligible; (3) the densities of the solid and liquid are equal; (4) the Boussinesq's assumption is valid for free convection, i.e. density variations are considered only insofar as they contribute to buoyancy, but are otherwise neglected; (5) the solid PCM is fixed to the container wall at all times. The last assumption is made only for the purpose of the present numerical study.

Based on the above assumptions and the enthalpy–porosity model [25,26], the governing equations in tensor form are as follows:

$$u_{i,i} = 0 \tag{1}$$

$$\rho\left(\frac{\partial u_i}{\partial t} + u_j u_{i,j}\right) = -p_{,i} + [\mu(u_{i,j} + u_{j,i})]_{,j} - \rho g_i \beta(T - T_0) + A u_i \tag{2}$$

$$\rho\left(\frac{\partial h}{\partial t} + u_j T_{,j}\right) = (kT_{,j})_{,j} \tag{3}$$

In Eq. (2)

$$A = -C(1 - \lambda)^2/(\lambda^3 + b) \tag{4}$$

in which b is a small constant introduced to avoid division by zero and C is a constant accounting for the morphology of the mushy region. In general, b is assigned a value of 0.001. For an isothermal phase change, C is assigned a value of 1.6×10^6.

The initial and boundary conditions are:

initial conditions:

$$T(x,0) = T^0(x)$$

$$u_i(x,0) = u_i^0(x) \tag{5}$$

boundary conditions:

$$u_i = \bar{u}_i(s,t) \quad \text{on } \Gamma_u$$

$$t_i = \sigma_{ij}n_j(s) = \bar{t}_i(s,t) \quad \text{on } \Gamma_t$$

$$T = \bar{T}(s,t) \quad \text{on } \Gamma_T$$

$$q = -(kT_{,j})n_j(s) = q_a(s,t) + q_c(s) + q_r(s) \quad \text{on } \Gamma_q \tag{6}$$

3. Charge of energy

An instantaneous temperature distribution in the PCM is obtained from the aforementioned mathematical equations. The magnitude of the cumulative energy charge per unit length, Q, is calculated as a function of time. This calculation is made by computing the enthalpy of the PCM at each time increment using the solid PCM at its fusion temperature as the reference state and then subtracting the enthalpy of the PCM at the beginning of the melting process. The value of Q is zero at the beginning and increases over the melting process toward Q_T, the cumulative energy charge for the whole melting process.

The maximum amount of energy which can be charged during the melting process is:

$$Q_M = \rho A_{xy}[f_H(T_w) - f_H(T_m)] \tag{7}$$

4. Dimensionless form of the governing equations in two dimensions

For convection-dominated two-dimensional melting or freezing problems subjected to the Dirichlet's boundary conditions, the dimensionless governing equations are:

solid region:

$$\frac{\partial H}{\partial Fo} = \frac{k_s}{k_l} Ste \left(\frac{\partial^2 \theta}{\partial X^2} + \frac{\partial^2 \theta}{\partial Y^2} \right) \tag{8}$$

liquid region:

$$\frac{\partial U}{\partial X} + \frac{\partial V}{\partial Y} = 0 \tag{9}$$

$$\frac{\partial U}{\partial Fo} + U\frac{\partial U}{\partial X} + V\frac{\partial U}{\partial Y} = -\frac{\partial P}{\partial X} + Pr\left(\frac{\partial^2 U}{\partial X^2} + \frac{\partial^2 U}{\partial Y^2}\right) + Ra\ Pr\ \sin\ \omega + A^*U \tag{10}$$

$$\frac{\partial V}{\partial Fo} + U\frac{\partial V}{\partial X} + V\frac{\partial V}{\partial Y} = -\frac{\partial P}{\partial Y} + Pr\left(\frac{\partial^2 V}{\partial X^2} + \frac{\partial^2 V}{\partial Y^2}\right) + Ra\ Pr\ \cos\ \omega + A^*V \tag{11}$$

$$\frac{\partial H}{\partial Fo} + U\frac{\partial H}{\partial X} + V\frac{\partial H}{\partial Y} = Ste\left(\frac{\partial^2 \theta}{\partial X^2} + \frac{\partial^2 \theta}{\partial Y^2}\right) \tag{12}$$

in which

$$H = \frac{c_s}{c_l}Ste\theta \quad \theta < 0$$

$$H = Ste\theta + 1 \quad \theta > 0 \tag{13}$$

and

$$U = \frac{u_x L_y}{\alpha_l} \quad V = \frac{u_y L_y}{\alpha_l} \quad \theta = \frac{T - T_m}{T_w - T_m} \quad H = \frac{h - c_s T_m}{\Delta h} \quad P = \frac{pL_y^2}{\rho\alpha_l^2}$$

$$X = \frac{x}{L_y} \quad Y = \frac{y}{L_y} \quad A^* = \frac{AL_y^2}{\rho\alpha_l} \quad Fo = \frac{t\alpha_l}{L_y^2} \quad Pr = \frac{c_l\mu}{k_l}$$

$$Ra = \frac{\rho^2 c_l g\beta L_y^3(T_w - T_m)}{\mu k_l} \quad Ste = \frac{c_l(T_w - T_m)}{\Delta h} \tag{14}$$

It is clear that melting and freezing heat transfer including free convection is determined by the following five dimensionless parameters; Rayleigh number (Ra), Prandtl number (Pr), Stefan number (Ste), the ratio of solid/liquid specific heat (c_s/c_l), as well as the ratio of solid/liquid thermal conductivity (k_s/k_l).

For melting of a solid PCM in a rectangular cavity with an isothermally heated wall, the dimensionless initial and boundary conditions are as follows:

initial conditions

$$\theta(X,Y,0) = \theta^0$$

$$U(X,Y,0) = V(X,Y,0) = 0 \tag{15}$$

boundary conditions

$U = V = 0$ on all the walls of the container

$\theta = \theta_{\text{B}}$ on an isothermal wall $\hspace{6cm}$ (16)

5. Validation of the model

The model is verified by comparison of the numerical prediction with the experimental results of Gau and Viskanta [7] and the implicit finite difference results of Lacroix [12] for the melting of a pure metal (gallium) inside a two-dimensional rectangular cavity (height $L_y = 0.0445$ m; width $L_x = 0.089$ m). The top and bottom boundaries are adiabatic. At time $t = 0$, the temperature of the left vertical wall is suddenly raised to a prescribed temperature above the melting point. The values of the governing dimensionless numbers and aspect ratio are listed in Table 1 for the test problem.

Fig. 1 compares the predicted phase front with both the experimental results of Gau and Viskanta [7] and the finite difference prediction of Lacroix [12]. It is seen from this figure that the present model is in reasonably good agreement with the results of the references.

The discrepancy between the predicted phase front of the present model and the experimental results is due to two possible reasons. First, in the experiment, the solid showed an initial sub-cooling of approximately 2°C. This degree of sub-cooling is significant in the light of the fact that the heated wall was only 8°C higher than the melting temperature of gallium. The second reason is that it is difficult to impulsively heat the vertical wall to a desired temperature in reality. The discrepancy of predicted phase front between the present model and Lacroix's model is due to the difference of the numerical methods used. Lacroix used a front tracking method while this model uses a fixed-grid enthalpy–porosity approach to model the phase change effects.

6. Results and discussion

Using the above-described numerical model, simulation runs were carried out for melting of a pure PCM in a rectangular cavity with an isothermally heated vertical wall. The top and

Table 1
Parameters used in the accuracy test runs

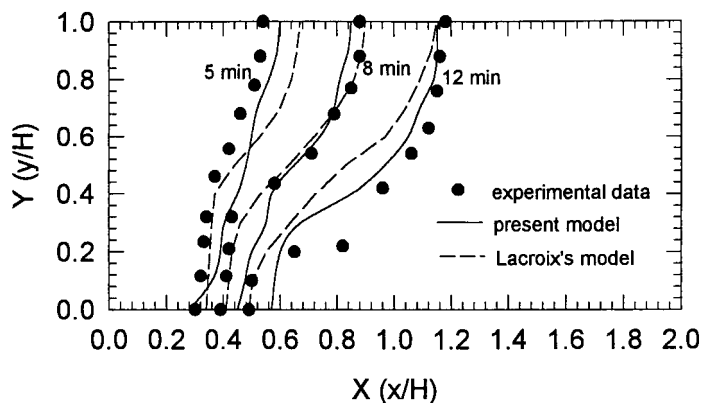|		
R	Aspect ratio, L_y/L_x	0.5
Ra	Rayleigh number	2.2×10^5
Pr	Prandtl number	0.021
Ste	Stefan number	0.042

Fig. 1. Comparison of the predicted phase front with experimental data.

bottom walls as well as the other vertical wall are assumed to be adiabatic. The parameters for the selected problem are listed in Table 2. The dimensional values were chosen to be within a realistic range for thermal energy storage of a sample PCM used (n-octadecane, 99% pure).

Grid-dependence tests indicated that the maximum difference for the dimensionless cumulative energy charge, Q_T/Q_M, is within 3.6% between using 20×20 elements with a dimensionless time step of 4.32×10^{-5} and 30×30 elements with the same time step, while the difference is only 1.5% between using 30×30 elements with a dimensionless time step of 4.32×10^{-5} and 40×40 elements with a time step of 2.16×10^{-5}. Therefore, 30×30 elements with a dimensionless time step of 4.32×10^{-5} were used for this and all the subsequent computations considering both accuracy and computing time.

Fig. 2 shows the predicted streamlines (Fig. 2(a)) and isotherms (Fig. 2(b)) at various Fo for the simulated problem. As expected, the flow pattern has just one recirculation in the melt zone. In Fig. 2(b4) and 2(b5), the isotherms are almost parallel. Such thermal stratification greatly decreases free convection and, therefore, the heat transfer rate.

Fig. 3 presents the variation of the dimensionless cumulative energy charge as a function of dimensionless time. This figure shows that the dimensionless cumulative energy charge increases linearly during the first half of the melting process. Afterwards, the charge rate begins to decrease. This is mainly caused by the thermal stratification mentioned earlier. At the second stage of the melting process only a small part of the solid remains at the bottom of the

Table 2
Parameters used in the simulation runs

R	Aspect ratio, L_y/L_x	1.0
Ra	Rayleigh number	2.844×10^6
Pr	Prandtl number	46.1
Ste	Stefan number	0.138
c_s/c_1	Ratio of solid/liquid specific heat	0.964
k_s/k_1	Ratio of solid/liquid heat conductivity	2.419
θ_i	Initial dimensionless temperature	-0.0256

(a1) $Fo = 0.108$ (b1) $Fo = 0.108$

(a2) $Fo = 0.194$ (b2) $Fo = 0.194$

(a3) $Fo = 0.302$ (b3) $Fo = 0.302$

(a4) $Fo = 0.432$ (b4) $Fo = 0.432$

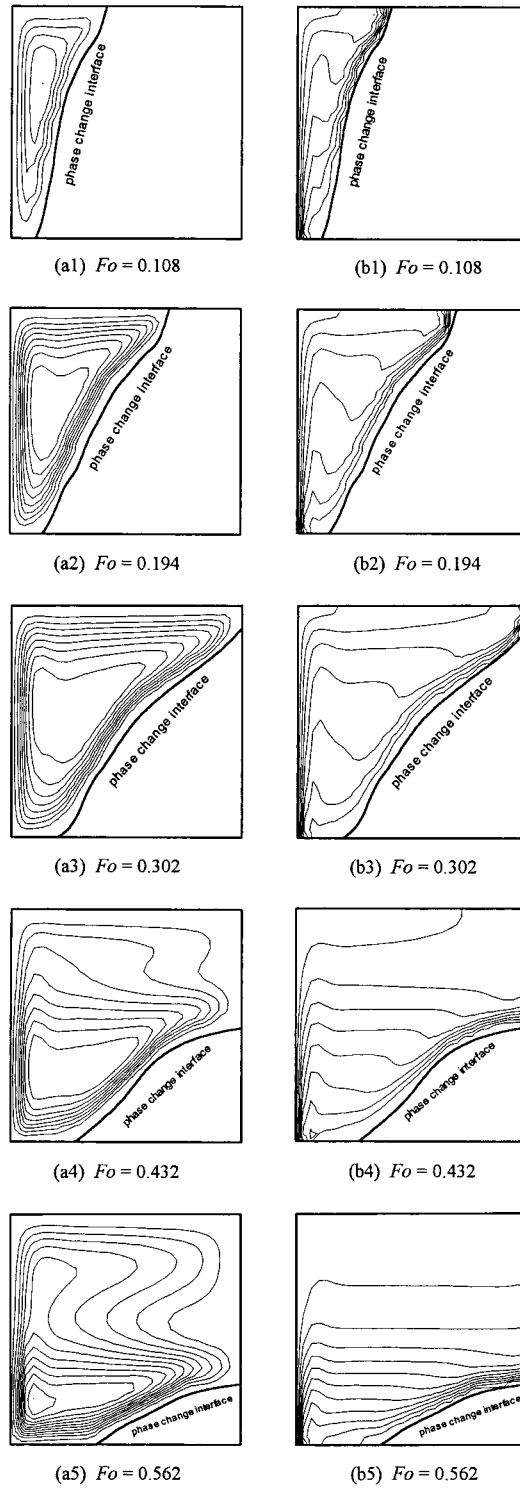(a5) $Fo = 0.562$ (b5) $Fo = 0.562$

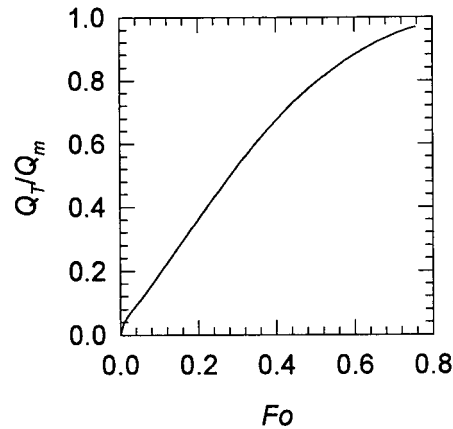Fig. 2. Streamlines and isotherms for melting with an isothermally heated vertical wall.

Fig. 3. Dimensionless energy charge curve.

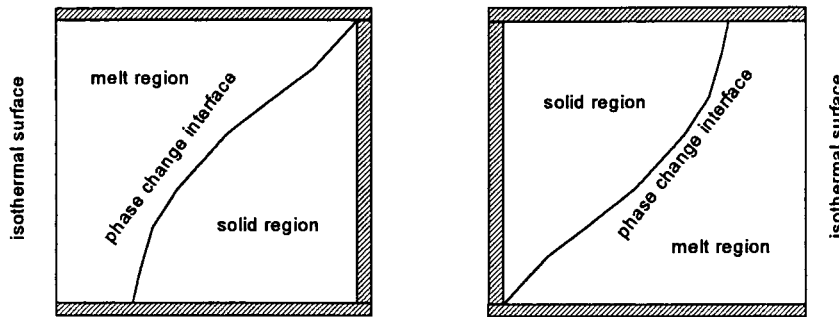Fig. 4. Schematic diagram of the physical system studied.

container. Thermal stratification occurs and significantly decreases the temperature gradient at the phase change interface and, therefore, the phase change heat transfer rate.

To enhance the heat transfer rate during the second half of the melting process, it is proposed to invert the PCM container once the phase change interface reaches the right vertical wall of the container. A schematic sketch representing this idea is shown in Fig. 4.

Simulations were carried out to investigate by how much the heat transfer rate can be enhanced by inverting the PCM container and what parameters influence the enhancement of heat transfer rate, if any. Due to extensive computing time requirements, no attempt is made to perform a complete parametric study of this problem. Only the effects of Rayleigh number (Ra) and Stefan number (Ste) on the enhancement of heat transfer during melting of a PCM are investigated. It should be noted that no difference in enhancement has been observed for Prandtl numbers larger than 10. For $Pr > 10$, the hydrodynamic boundary layer is already much thicker than the thermal boundary layer and thus further increase in Pr makes no difference in the convective hydrodynamic and thermal fields.
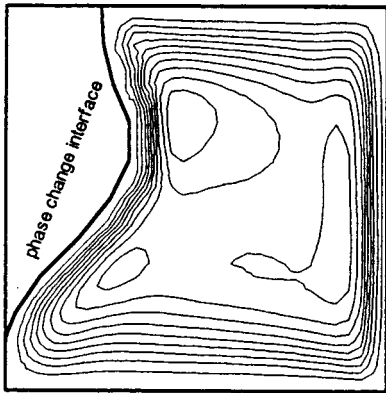
It is reasonable to assume that the liquid phase is well mixed and the melt is stationary upon
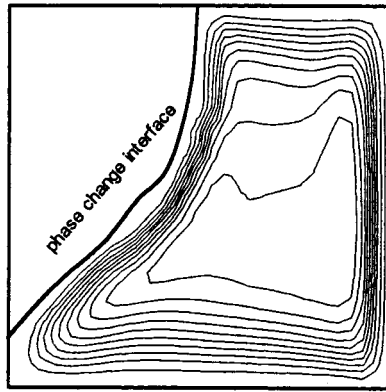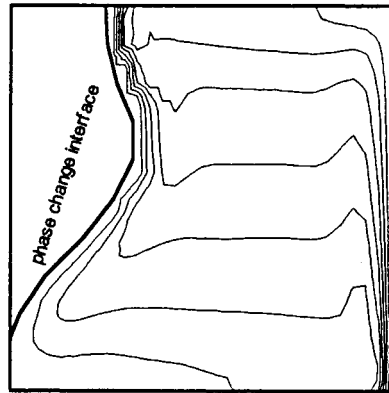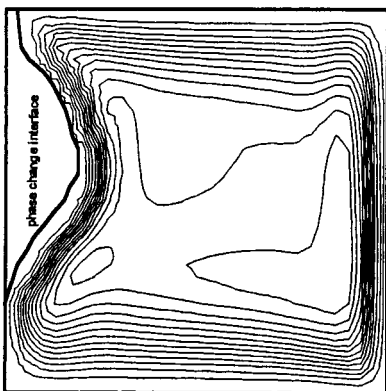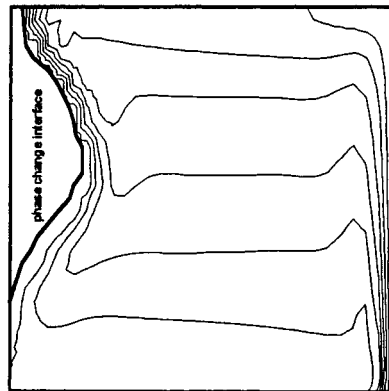
(a1) *Fo* = 0.367

(b1) *Fo* = 0.367

(a2) *Fo* = 0.432

(b2) *Fo* = 0.432

(a3) *Fo* = 0.497

(b3) *Fo* = 0.497

Fig. 5. Streamlines and isotherms for inverted PCM container.

inverting the PCM container. Numerical experiments indicated that whether or not the liquid phase is assumed to be well mixed and stationary has little effect on the resulting heat transfer. This is due to the fact that the formation of convective flows in the melt from stationary state requires a very short time compared with the total heat transfer process simulated. Therefore, in subsequent simulations, the temperature and velocity fields were not modified after the container is inverted.

6.1. Effects of Rayleigh number on the enhancement of phase change heat transfer rate

Three cases were computed to investigate the effects of Rayleigh number on enhancement of the energy charge rate by inverting the PCM container. All the parameters used in this investigation are held constant and identical to those listed in Table 2 except for the Rayleigh number. Table 3 shows the computed cases and comparison of the energy charge rates at different Rayleigh numbers. In this table, the 'first period' designates the period before inverting the container and the 'second period' refers to conditions after the container is inverted.

From Table 3 it is seen that the energy charge rate can be enhanced 56.5% in the 'second period' simply by inverting the PCM container for the case of Rayleigh number equal to 2.844×10^6. It is seen also that enhancement of the heat transfer rate increases with an increase in Rayleigh number. This is due to the fact that the larger the Rayleigh number the larger the role free convection plays in melting phase change heat transfer. Since heat transfer is mainly conduction-dominated during the second stage of the melting process in the case of non-inverted container, increasing Rayleigh number hardly improves the melting heat transfer rate. However, in the case of inverted PCM container, the 'second period' of the melting process is mainly controlled by free convection. Therefore, with an increase in Rayleigh number, the melting heat transfer rate increases.

Displayed in Fig. 5 are the predicted streamlines and isotherms at different dimensionless times (Fourier numbers) for the 'second period' in the case of inverted PCM container for Rayleigh number equal to 2.844×10^6. It is seen from Fig. 5(b1)–(b3) that no obvious thermal stratification occurs at the second stage of the melting process. Due to this fact, the role which free convection plays does not diminish during the second stage of the melting process. This explains why the energy charge rate is enhanced by inverting the PCM container.

Table 3
Effects of Rayleigh number on energy charge rate

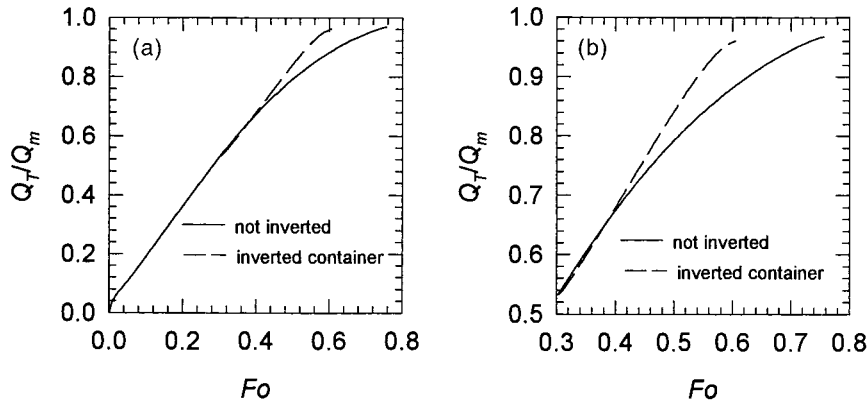| Ra	First period		Second period, $(\Delta Q/Q_M)/\Delta Fo$		
	$\Delta Q/Q_M$	Fo	No inverting	Inverting	Enhancement
7.11×10^5	0.582	0.302	0.687	1.047	52.4%
2.844×10^6	0.532	0.467	0.961	1.504	56.5%
5.688×10^6	0.515	0.251	1.099	1.766	60.1%

Fig. 6. (a) Comparison of dimensionless cumulative energy charge. (b) An amplification of Fig. 6(a).

Fig. 6(a) compares the dimensionless cumulative energy charge curves between the two cases of inverted and non-inverted cases. Fig. 6(b) is an amplification of Fig. 6(a) for the 'second period' of the melting process (after $Fo = 0.302$). In Fig. 6(a), the energy charge curves for inverted and non-inverted cases are identical before $Fo = 0.302$. This is because the inverting action is taken after $Fo = 0.302$. From Fig. 6(a), no obvious slow-down in the energy charge rate is seen for the case of inverted PCM container during the second stage of the melting process.

Fig. 7 presents comparison of the dimensionless cumulative energy charge curves at different Rayleigh numbers corresponding to the computed cases in Table 3 for both inverted and non-inverted cases. It is seen from this figure that, for both cases, the larger the Rayleigh number the higher the energy charge rate.
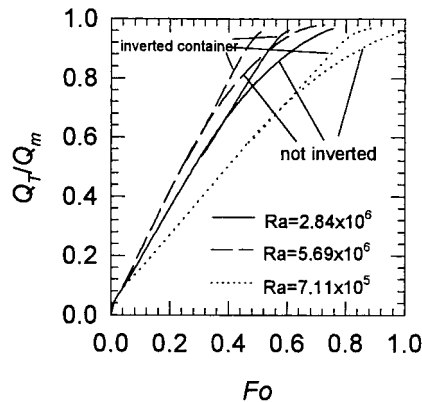

Fig. 7. Effects of Rayleigh number on energy charge rates: comparison of Q_T/Q_M for inverted and non-inverted containers.

Table 4
Effects of Stefan number on energy charge rate

Ste	First period		Second period, $(\Delta Q/Q_M)/\Delta Fo$		
	$\Delta Q/Q_M$	Fo	No inverting	Inverting	Enhancement
0.138	0.532	0.302	0.961	1.504	56.5%
0.552	0.543	0.147	2.172	2.928	34.8%
1.104	0.481	0.0864	3.598	4.279	18.9%

6.2. Effects of Stefan number on the enhancement of heat transfer rate

Three cases were computed to investigate the effects of the Stefan number on the enhancement of the energy charge rate by inverting the PCM container. All the parameters used in this investigation are held constant and identical to those listed in Table 2 except for variation of the Stefan number. Table 4 shows the computed cases and comparison of the energy charge rates among different Stefan numbers. From this table, it is clear that the larger the Stefan number the smaller the enhancement of the energy charge rate. This is mainly due to the fact that the larger the Stefan number the smaller the latent heat effects. In the limiting case of $Ste \to \infty$, i.e. the latent heat is equal to zero and the PCM can be taken as a liquid. Inverting the container of a liquid has little effect on convection heat transfer rate when heated at the side wall of the container.

7. Concluding remarks

Melting of a phase change material in a rectangular enclosure with an isothermally heated vertical wall was simulated. To enhance the heat transfer rate, inverting the PCM container at an appropriate stage in the melting process is proposed as a novel yet simple idea which was investigated numerically. Numerical experiments showed that the heat transfer rate can be greatly improved by inverting the PCM container. The magnitude of the enhancement of the heat transfer rate varies with Rayleigh number and Stefan number. This idea can be implemented in new PCM thermal energy storage devices. If a full inversion is not practicable in some applications, it is also possible to tilt the container by a few degrees to achieve some enhancement.

References

[1] N.W. Hale, R. Viskanta, Photographic observation of the solid–liquid interface motion during melting of a solid heated from an isothermal vertical wall, Lett. Heat Mass Transfer 5 (1978) 329–337.
[2] P.D. Van Buren, R. Viskanta, Interferometric measurement of heat transfer during melting from a vertical surface, Int. J. Heat Mass Transfer 23 (1980) 568–571.

[3] M. Okada, Melting from a vertical plate between insulated top and bottom surfaces, in: Proceedings of ASME/JSME Thermal Engineering Joint Conference, Vol. 1, 1983, pp. 281–288.

[4] M. Bareiss, H. Beer, Experimental investigation of melting heat transfer with regard to different geometry arrangements, Int. Commun. Heat Mass Transfer 11 (1984) 323–333.

[5] C.J. Ho, R. Viskanta, Heat transfer during melting from an isothermal vertical wall, J. Heat Transfer 106 (1984) 12–19.

[6] C. Benard, D. Gobin, F. Martinez, Melting in rectangular enclosures: experiments and numerical simulations, J. Heat Transfer 107 (1985) 794–803.

[7] C. Gau, R. Viskanta, Melting and solidification of a pure metal on a vertical wall, J. Heat Transfer 108 (1986) 174–181.

[8] F. Wolff, R. Viskanta, Melting of a pure metal from a vertical wall, Exp. Heat Transfer 1 (1987) 17–30.

[9] M. Okada, Analysis of heat transfer during melting from a vertical wall, Int. J. Heat Mass Transfer 27 (1984) 2057–2066.

[10] A. Gadgial, D. Gobin, Analysis of two-dimensional melting in rectangular enclosures in presence of convection, J. Heat Transfer 106 (1985) 20–26.

[11] B.W. Webb, R. Viskanta, Analysis of heat transfer during melting of a pure metal from an isothermal vertical wall, Numer. Heat Transfer 9 (1986) 539–558.

[12] M. Lacroix, Predictions of natural convection-dominated phase change problems by the vorticity–velocity formulation of the Navier–Stokes equations, Numer. Heat Transfer, Pt B 22 (1992) 79–93.

[13] M. Costa, A. Oliva, C.D. Perez Segarra, R. Alba, Numerical simulation of solid–liquid phase change phenomena, Comput. Meth. Appl. Mech. Engng 91 (1991) 1123–1134.

[14] A.S. Usmani, R.W. Lewis, K.N. Seetharamu, Finite element modeling of natural convection-controlled change of phase, Int. J. Numer. Meth. Engng 14 (1992) 1019–1036.

[15] M.A. Rady, A.K. Mohanty, Natural convection during melting and solidification of pure metals in a cavity, Numer. Heat Transfer, Pt A 29 (1996) 49–63.

[16] J.R. Keller, T.L. Bergman, Prediction of conjugated heat transfer in solid–liquid system: inclusion of buoyancy and surface tension forces in the liquid phase, J. Heat Transfer 111 (1989) 690–698.

[17] T.L. Bergman, B.W. Webb, Simulation of pure metal melting with buoyancy and surface tension forces in the liquid phase, Int. J. Heat Mass Transfer 33 (1990) 139–149.

[18] A. Liu, T.E. Voth, T.L. Bergman, Pure metal melting and solidification with liquid phase buoyancy and surface tension forces, Int. J. Heat Mass Transfer 36 (1993) 411–422.

[19] C.J. Ho, C.H. Chu, Periodic melting within a square enclosure with an oscillatory temperature, Int. J. Heat Mass Transfer 36 (1993) 725–733.

[20] C.J. Ho, C.H. Chu, The melting process of ice from a vertical wall with time-periodic temperature perturbation inside a rectangular enclosure, Int. J. Heat Mass Transfer 36 (1993) 3171–3186.

[21] C.J. Ho, C.H. Chu, Numerical simulation of heat penetration through a vertical rectangular phase change material/air composite cell, Int. J. Heat Mass Transfer 39 (1996) 1785–1795.

[22] B.W. Webb, R. Viskanta, Natural-convection-dominated melting heat transfer in an inclined rectangular enclosure, Int. J. Heat Mass Transfer 29 (1986) 183–192.

[23] H. Inaba, M. Nagaya, T. Fukuda, M. Sugawara, A study on transient characteristics of melting phase change material in inclined rectangular heat storage enclosures, Trans. JSME 57B (1989) 200–205.

[24] H. Inaba, S. Morita, M. Nagaya, S. Nozu, Numerical study on heat storage characteristics of inclined rectangular latent heat storage, Trans. JSME 55B (1992) 2555–2564.

[25] V.R. Voller, C. Prakash, A fixed grid numerical modelling methodology for convection–diffusion mushy region phase-change problems, Int. J. Heat Mass Transfer 30 (1987) 1709–1719.

[26] A.D. Brent, V.R. Voller, K.J. Reid, Enthalpy–porosity technique for modelling convection–diffusion phase change: application to the melting of a pure metal, Numer. Heat Transfer 13 (1988) 297–318.